Motional resonance coupling in cold multispecies Coulomb crystals

B. Roth, P. Blythe, and S. Schiller
Institut für Experimentalphysik, Heinrich-Heine-Universität Düsseldorf, 40225 Düsseldorf, Germany
(Received 24 August 2006; published 1 February 2007)

We investigate the coupling between motional resonances of translationally cold (10 mK range) atomic and molecular ions in multispecies Coulomb crystals, stored in a linear Paul trap. The atomic and molecular ions were sympathetically cooled by laser-cooled Be^+ ions. The motional resonances of the different ion species were determined nondestructively with high mass-to-charge resolution upon excitation with an oscillating electric field. The experimental results show good agreement with results from molecular dynamics simulations and allow for a precise identification of sympathetically cooled particles in multispecies ion crystals.

DOI: 10.1103/PhysRevA.75.023402 PACS number(s): 32.80.Pj, 52.27.Jt, 52.27.Gr, 61.50.−f

I. INTRODUCTION

There is a growing body of research focused on the production of dense samples of cold gas phase molecules, which are of interest in chemical physics, molecular physics, and plasma and astrophysics among other fields. Trapped ensembles of cold molecules are promising systems for the study and control of chemical reactions. High-precision measurements of fundamental constants may also be enhanced or enabled by using cold trapped molecular ions [1,2].

For neutral species, several methods for cold molecule production have been demonstrated. These include the formation of alkali-metal dimers from precooled atoms via Feshbach resonances or photoassociation [3–5], and trapping and cooling of preexisting molecules using buffer gas cooling or static electric fields [6,7]. For molecular ions, sympathetic cooling has been used to cool a large variety of molecular species via their interaction with cold atomic ions in electrostatic or electrodynamic ion traps [8,9]. In such a situation, the translational molecular motion may be reduced to a few tens of millikelvin, or less, by interaction with laser-cooled (LC) atomic ions.

The development of techniques for the production of cold molecules also requires the development of particle identification techniques. In general, fluorescence detection is not applicable due to the lack of closed transitions. Time-of-flight mass spectroscopy is a destructive method for molecular ions or after ionization of neutral molecules. Nondestructive techniques are of interest because they can increase the experimental flexibility. The excitation of the mass-dependent motional resonances of the trapped ions is one such technique, and is widely used for mass spectrometry of large and small ion clouds [10–12].

We have used excitation of motional resonances to identify the molecular species embedded in laser-cooled crystals of beryllium ions [9]. In the crystalline state mutual Coulomb interactions are dominant and, therefore, the motional resonance spectrum is more complicated than for ion clouds (fluid state). The interactions between the different ion species can perturb the observed motional frequencies by a significant amount. In this work, we analyze such perturbations both experimentally and via molecular dynamics (MD) simulations. We consider multicomponent ion crystals containing up to several thousand Be^+ ions with fractions of sympathetically cooled (SC) ions of up to 70%. The results obtained increase our ability to unequivocally identify the species present in the ion trap, and lead directly to increased sensitivity for spectroscopic and chemical experiments on cold, trapped molecular ions.

II. BASIC TRAP THEORY

For a linear radio-frequency ion trap (Paul trap), the axial (ω_z) and radial (ω_r) secular frequencies of an ion species in the harmonic effective trap potential (pseudopotential) $U_{trap}(x,y,z)=(m/2)(\omega_r^2 r^2+\omega_z^2 z^2)$ are given by $\omega_z=(2\kappa Q V_{EC}/m)^{1/2}$ and $\omega_r=(\omega_0^2-\omega_z^2/2)^{1/2}$, respectively, with $\omega_0=QV_{rf}/\sqrt{2}m\Omega r_0^2$ and $r^2=x^2+y^2$. The z axis is along the centerline of the trap and $\kappa\approx 3\times 10^{-3}$ mm^{-2} is a constant determined by the trap geometry. Q and m are the mass and the charge of the trapped ion species, V_{rf} and Ω are the amplitude and the frequency of the rf driving field (for radial confinement of the particles), and V_{EC} is a dc potential giving the longitudinal confinement along the z axis. r_0 is the distance from the electrode surfaces to the trap axis.

It can be seen from the above expressions that simple scaling laws apply for the radial oscillation frequencies of single trapped ions, namely, that $\omega_r \propto q/m$ for $|a_r|=4QV_{dc}/mr_0^2\Omega^2 \ll |q_r|=2QV_{rf}/mr_0^2\Omega^2$ and $\omega_0 \gg \omega_z$. Here, V_{dc} is a static quadrupole potential on the trap electrodes. For singly charged ions, as studied here, simple ratios are expected between the motional frequencies of different trapped species, if the coupling between the species is neglected. The oscillation frequencies reflect the strength of confinement, and so lighter ions will generally be closer to the trap axis than heavier ions. This radial separation is seen clearly for multispecies ion crystals [8,9].

III. EXPERIMENT

The trap used in these experiments is driven at 14.2 MHz, with a peak-to-peak rf amplitude of 380 V, enclosed in an ultrahigh-vacuum chamber. The chamber is equipped with a leak valve for the controlled introduction of neutral molecules.

Beryllium atoms are evaporated from an oven, and ionized in the trap center by a 750 eV electron beam, where they are laser-cooled to a few millikelvin. Experimentally,

we find that the relatively large value for the electron beam energy is favorable for efficient loading of beryllium ions to our trap. The cooling laser light, resonant with the $^2S_{1/2}(F=2) \rightarrow {}^2P_{3/2}$ Be^+ transition at 313 nm, is produced by doubly resonant sum frequency generation [13]. An acousto-optic modulator allows for tuning of the uv frequency within a range of 340 MHz. Optical pumping to the metastable $^2S_{1/2}(F=1)$ ground state is prevented by generating 1.25 GHz sidebands on the cooling light via an electro-optic modulator. The fluorescence of the Be^+ ions is measured with a photomultiplier tube and a charge-coupled device (CCD) camera. The camera integration time was 2 s.

The laser cooling leads to a phase transition from a disordered cloud or "cold fluid" to an ordered state, a Coulomb crystal [14,15]. Typical translational temperatures of the crystallized beryllium ions are well below 20 mK [16]. For definition of a quantization axis, a magnetic field of a few gauss is applied to the trap (along its z axis). This low field does not perturb the motion of the ions at any detectable level.

IV. TRAP LOADING

The loading of beryllium ions typically also produces ions of the residual gas in our vacuum chamber—mostly N_2^+. Some of these heavier ions collect outside the beryllium ion ensemble. Mass-selective cleaning of the trap is applied to eject these heavy impurity ions. To this end, we temporarily add a static quadrupole potential V_{dc} to the trap electrodes, breaking the radial symmetry [17]. As V_{dc} increases, heavier ions are no longer stable in the trap and are ejected. In this way we can efficiently remove all heavy impurity ions.

Subsequently, molecular ions are loaded into the trap by leaking neutral molecules into the vacuum chamber and ionizing them with the electron beam energy set to below 200 eV. The neutral gases used for the experiments detailed here are ^3He, ^4He, H_2, HD, and D_2. The primary ions produced from these gases are lighter than beryllium, and these ions collect in the center of the trap, forming a dark (nonfluorescing) core in the beryllium crystal. After loading the molecular ions, motional excitation scans, detailed below, are performed.

V. METHODS

In order to identify the trapped ion species we excite the radial motion of the ions in the trap using an external plate electrode to which an oscillating electric field is applied. The electrode is placed at 45° to the x and y axes of the trap, perpendicular to the z axis. The z axis is horizontal, parallel to the cooling laser beam direction. The excitation field has an amplitude of up to several volts and its frequency is scanned between 2 kHz and 2 MHz.

When the excitation field is resonant with the oscillation mode of a crystal component, energy is pumped into the motion of that component. Via the Coulomb interaction, some of this energy is eventually distributed through the crystal as heat, increasing the temperature of the beryllium ions. This modifies the fluorescence intensity of the beryllium ions. For the motional excitation spectra presented here, the cooling laser was detuned to the red of the beryllium fluorescence line center by two to three natural linewidths (40–60 MHz). In this case, increasing the temperature of the beryllium ions leads to an increase in the observed fluorescence (and also to an increase in the cooling rate, limiting the temperature rise). Thus, the beryllium fluorescence level as a function of excitation frequency indicates the motional spectrum of all ions.

VI. COUPLING MECHANISMS AND RESULTS

The equations given above for the motional frequencies of a single ion in a harmonic trap are also valid for the center-of-mass motion of large, single-species ion crystals, as confirmed in experiment. However, mixed-species crystals can complicate this picture. The motion of each species is then affected by the Coulomb potential of all the others. In multicomponent ion plasmas containing several different ion species, the coupling between the motional modes of the different ion species can depend strongly on the temperature of the ion plasma (and thus on its state, fluid or crystalline). In order to characterize the different coupling mechanisms we compare the spectra of multispecies ion crystals with those in the fluid state, where coupling between different ion species is much weaker due to the larger interparticle spacing.

The spatial distribution of the ion species can then also affect the motional frequencies and the strength of coupling between them. Strong effects are, for example, seen when a static offset potential is present in the trap, such that the equilibrium positions of the ions are displaced from the trap center. Finally, the motional spectra exhibit systematic shifts related to the excitation method, requiring their characterization.

A. Systematics

1. Scan amplitude

As a simple two-component system, a Be^+ crystal was loaded with $^4He^+$ ions [Fig. 1(a)]. Helium ions are used here, because during the loading of helium isotopes, only small amounts of impurity ions are formed. Since these ions collect in the outer shells of the ion crystal they can easily be removed by temporary application of a dc quadrupole potential. Figure 1(a) shows the crystal used for the above measurements containing ≈ 1100 Be^+ and ≈ 250 $^4He^+$. The observed crystal structure is in good agreement with results from MD simulations, Fig. 1(b). The Be^+ and He^+ ions have a translational temperature of ≈ 15 mK, as found by fitting an appropriate Voigt profile to the Be^+ line obtained by a frequency scan of the cooling laser over the atomic resonance and by the MD simulations, assuming equal heating rates for both species [9,16].

Repeated motional excitation was performed, with increasing excitation amplitude from 0.5 to 4 V. Figure 1(c) illustrates the shift of the observed motional frequencies caused by variations in the excitation amplitude. The fit to the experimental data gives a coefficient of the shift of the

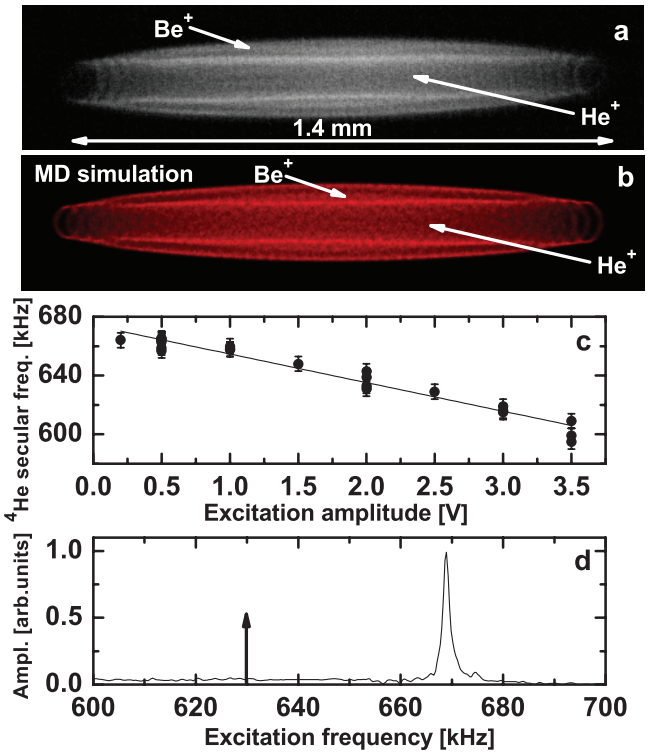

FIG. 1. (Color online) Drive-amplitude-induced resonance frequency shift. (a) Two-component Be^+-$^4He^+$ ion crystal underlying the measurement, containing ≈1100 Be^+ and ≈250 $^4He^+$ ions. Cooling laser direction is to the right. (b) MD simulation of the ion crystal in (a). (c) Motional frequencies for ultracold $^4He^+$ ions for the above ion crystal as a function of excitation amplitude. The line is a linear fit to the data. (d) Simulated secular frequency spectrum for the crystal in (b). Note that the $^4He^+$ secular frequency for zero excitation amplitude in (c), (d) is shifted to higher values compared to the calculated single-particle frequency (at 630 kHz), which is marked by a vertical arrow.

resonance frequency of ≈−20 kHz/V for $^4He^+$ (possible small nonlinear contributions to this behavior will be investigated in more detail in future studies). This shift can be explained by the interplay between two competing effects, the species-dependent cooling and heating rates present in the trap (see [18] for a detailed discussion).

Figure 1(d) shows the simulated secular frequency spectrum for the crystal shown in Fig. 1(b). The secular excitation process is simulated by instantly shifting the particles in one radial direction, e.g., the x direction, which then subsequently perform oscillations around their equilibrium positions, damped by the interactions. Via MD simulations (without micromotion of the ions taken into account), the position of each particle is computed versus time. A Fourier analysis of the total kinetic energy time series gives the secular oscillation spectrum [19]. For the simulated spectrum, where a (relatively) small initial position shift is applied, the $^4He^+$ feature appears at 670 kHz. For comparison, the calculated single-particle frequency for $^4He^+$ is at 630 kHz. This shift agrees well with the extrapolated experimental value of 675 kHz from Fig. 1(c). Details on the numerical code can be found in [19]. See below for a discussion of the upward shift observed.

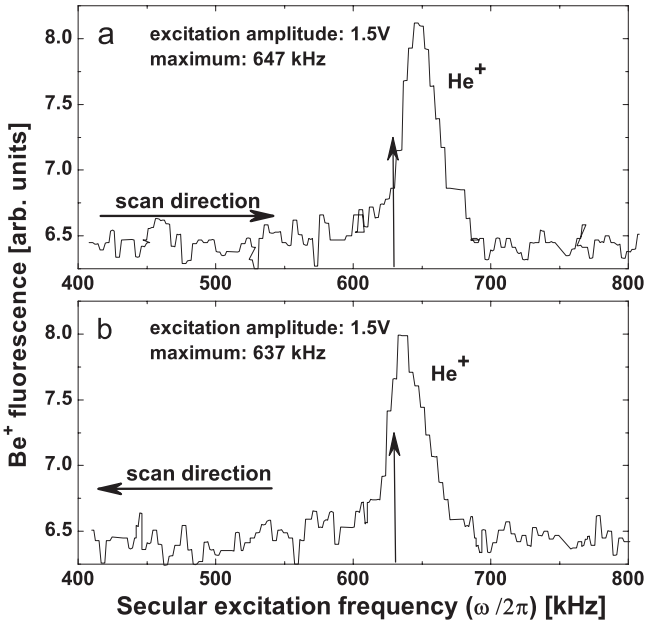

FIG. 2. Scan-direction-induced resonance frequency shift: Motional frequency spectrum of an cold Be^+ ion crystal (<20 mK) loaded with He^+ ions. Sweep direction toward higher (a) and toward lower (b) frequencies. The calculated single-particle secular frequency for $^4He^+$ ions is marked by vertical arrows.

2. Scan direction

Another shift of the observed frequency is related to sweep direction of the motional excitation scan, shown in Fig. 2. An explanation for this effect can also be found in [18]. The $^4He^+$ resonance in backward direction is shifted toward smaller values compared to the forward scan by ≈10 kHz, this value being roughly constant across excitation amplitudes.

VII. INTERACTION-INDUCED FREQUENCY SHIFTS

A. Strong coupling

Strong coupling between trap modes of two different SC ion species contained in a Be^+ crystal is illustrated in Fig. 3(a). The mixed-species Be^+ ion crystal was formed following inlet and ionization of neutral H_2 gas. During the inlet phase, the neutral H_2 gas can react with H_2^+ ions to produce H_3^+ ions. This reaction proceeds with a large reaction rate on the order of the Langevin rate, with a rate constant $k=2.9\times10^{-9}$ cm^3/s [20–22]. The inset in Fig. 3(a) shows the mixed-species ion crystal observed, with the large dark core stemming from the embedded light molecular ions. The slight asymmetry of shape of the crystal is due to small anisotropies of the effective trap potential and smaller amounts of heavier BeH^+ ions outside the Be^+ ion shells.

With large numbers of H_3^+ and H_2^+ ions, forming a multi-shelled core in the Be^+ crystal, their radial motions can be strongly coupled. In this situation, the ions of different species are sufficiently tightly coupled that they all oscillate at the same frequency. The situation is made more complex by the inhomogeneous environment of each ion, such as its po-

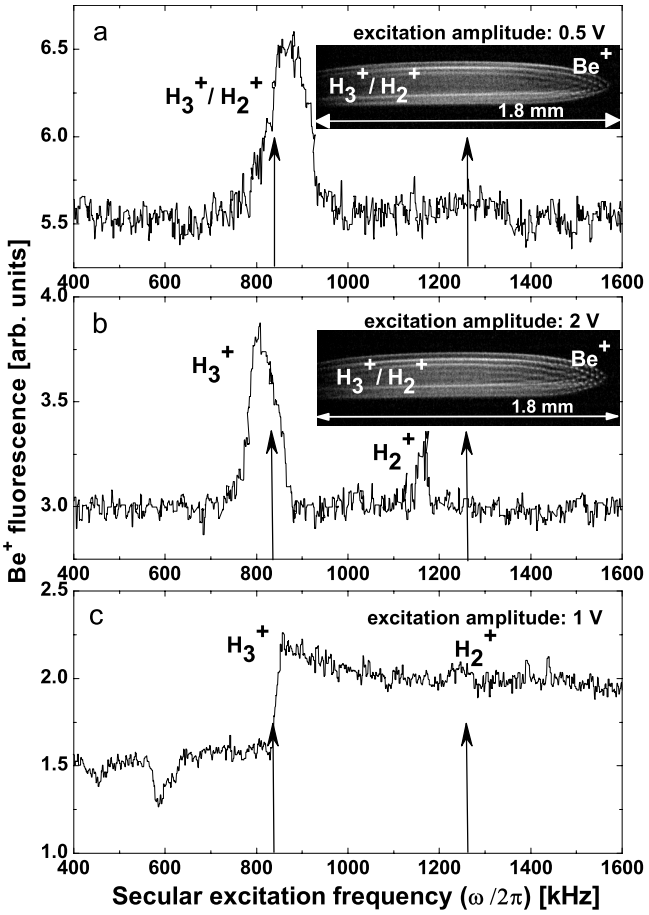

FIG. 3. Interaction-induced strong (a), (b) and weak (b) coupling, (a) Motional frequency spectrum of a Be^+ ion crystal following electron impact ionization of H_2 gas. The crystal (see inset) contains ≈1400 LC Be^+ ions and ≈1300 SC ions (as found by MD simulations). The SC ions consist of ≈700 H_2^+ and H_3^+ ions, located in the crystal core, and of ≈600 BeH^+ ions located outside the Be^+ shells. The latter are responsible for the slight asymmetry in the shape. The translational temperature of all species is ≈20 mK. Sweep direction toward higher frequencies. (b) Motional spectrum and ion crystal (inset) after partial removal of lighter SC ions (note the reduced size of the core), containing ≈1350 LC ions and ≈1200 SC ions: ≈450 H_3^+, ≈100 H_2^+, and ≈650 BeH^+. Relative fractions for the light ions were estimated from the size of the features in the spectrum. (c) Spectrum following electron impact ionization of H_2 gas in the cloud state. Calculated single-particle secular frequencies for the SC ions are marked by arrows: 840 kHz (H_3^+) and 1260 kHz (H_2^+). The feature at ≈580 kHz is attributed to the excitation of the second harmonic of the Be^+ trap mode (calculated frequency 560 kHz).

sition in the center or toward one end of the crystal. The individual positions can be strongly affected by the exact composition of the core. This leads to the spectrum seen in Fig. 3(a). The spectrum shows a broad feature between 800 and 930 kHz and was obtained with an excitation amplitude of 0.5 V. The calculated single-particle secular frequencies for pure H_3^+ or H_2^+ are at 840 and 1260 kHz, respectively.

For comparison, we also measured the secular spectrum for a mixed-species (Be^+, H_3^+, and H_2^+) ion plasma in the cloud (fluid) state [23], after loading and electron impact ionization of neutral H_2 gas, Fig. 3(c). The obtained secular frequencies for the individual species H_3^+ and H_2^+ are closer to the calculated single-particle value. This is due to the smaller coupling between the different ion species as compared to the crystalline state. At the excitation amplitude used, 1 V, a fraction of the SC ions was expelled from the trap when scanning over the H_3^+ secular frequency, by heating their translational motion. As a consequence of the removal of SC ions, the ion plasma becomes colder, but still remains in the cloud state, and the Be^+ fluorescence increases. After the scan has passed the H_3^+ resonance frequency, a slow decrease of the fluorescence occurs, probably, due to LC and SC ions reaching thermal equilibrium. Therefore, the secular spectrum [Fig. 3(c)] shows a steplike feature at this frequency, in contrast to the situation in the crystalline state. However, this reduction of temperature in the mixed-species ion plasma subsequently leads to a decrease of the H_2^+ feature in the secular spectrum, compared to the crystalline case [Fig. 3(a)]. In general, for a given ion number ratio, we found that the size of a specific spectral feature is, in first order, proportional to the excitation amplitude and inversely proportional to the ion temperature, for both the fluid and crystalline state.

The decrease in Be^+ fluorescence at around 580 kHz in Fig. 3(c) is attributed to the excitation of the second harmonic of the Be^+ trap mode of oscillation. This resonance is seen only in the cloud state and for slightly asymmetric trap potentials. The latter may also explain the shift of the Be^+ second harmonic frequency compared to the calculated frequency (560 kHz). According to the simulations, such an asymmetry-induced shift affects mainly the heavier ion species (Be^+) and is negligible for ion species closer to the trap axis (H_3^+ and H_2^+), due to their smaller mass-to-charge ratio and, consequently, the steeper trap potential.

The coupling strength between trap modes in mixed-species ion crystals can be controlled via the ion number ratio. Figure 4 shows a mixed-species ion crystal where the SC ion number ratio was varied [Figs. 4(a)–4(c)]. The crystal was obtained by loading and ionization of HD gas into a pure Be^+ ion ensemble. Initially, it contains ≈1000 Be^+ ions, ≈75 HD^+ ions, and ≈25 D^+ ions [Fig. 4(a)]. While repeated secular excitation measurements are performed [Figs. 4(d) and 4(e)], the number of HD^+ ions was decreased by dissociation using suitable lasers [24]. This leads to the formation of additional D^+ (and H^+) ions. Note that a part of the HD^+ dissociation product ions is lost from the trap, probably due to the large kinetic energy of these ions [24]. Furthermore, small background losses of both HD^+ and D^+ ions are due to chemical reaction with residual background gases. The initial HD^+ ion number was reduced to zero during the run, as obvious from the size reduction of the dark crystal core [Figs. 4(a)–4(c)] and the relative sizes of the individual features in the spectra [Fig. 4(e)]. At the same time, the number of D^+ ions is raised to ≈35. As more and more HD^+ ions are dissociated, the numbers and relative fractions of HD^+ and D^+ ions are varied, and thus the coupling between their trap oscillation modes is modified. Reduced coupling strength between the different HD^+ and D^+ trap modes enables their resolution in the spectra toward the middle of the run [Fig. 4(e)]. The results described also show the transition between strong (at the beginning of the run) and weak coupling of

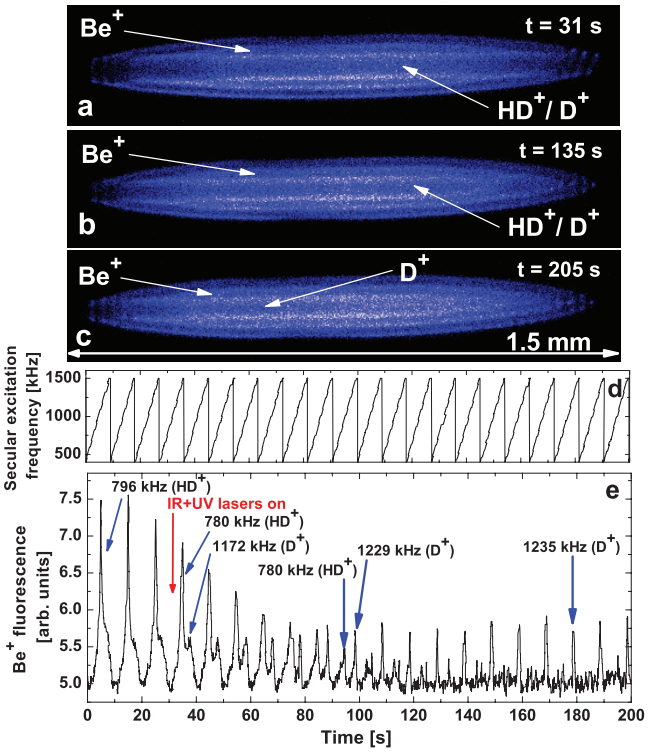

FIG. 4. (Color online) Coupling strength as a function of relative particle fractions. (a), (b), (c) Mixed-species ion crystal at three different times after the start of the secular frequency measurement, containing different ion numbers and relative particle fractions. The change of the ion numbers is obvious from the reduction in size of the crystal core (containing HD^+ and D^+ ions) with time. Ion species numbers obtained from simulations: (a) 1000 Be^+, 75 HD^+, and 25 D^+, (b) 1000 Be^+, 20 HD^+, and 30 D^+, (c) 1000 Be^+ and 35 D^+. (d) Repeated secular excitation frequency scans (scan range 400–1100 kHz). Sweep direction toward higher frequencies. Excitation amplitude 3 V. (e) Series of low-mass motional frequency spectra, illustrating the change of the strong coupling effect as a function of relative ion numbers. The measured resonance frequencies for HD^+ and D^+ ions for three times during the run are also shown.

trap modes (toward the end of the run). See below for a detailed discussion.

B. Weak coupling

Figure 3(b) shows the secular frequency spectrum after removal of a fraction of the SC ions, via repeated secular excitation. This leads to a reduction of the size of the dark crystal core, visible in the inset. The number of Be^+ and BeH^+ ions changed slightly compared to Fig. 3(a), due to chemical reactions with residual background H_2 gas [25,26].

In the spectrum, two resonances are now identified, attributed to the presence of H_3^+ and H_2^+ ions. The H_3^+ resonance, however, is shifted toward lower frequencies (by ≈30 kHz) compared to its single-particle frequency (at 840 kHz), whereas the H_2^+ resonance exhibits a larger shift (by ≈90 kHz) relative to its single-particle frequency at 1260 kHz. The positions of the resonances are determined by two mechanisms, a downward frequency shift caused by the amplitude of the motional excitation combined with an upward shift which is intrinsic to the situation of more than one species being simultaneously trapped [27]. The resulting shift of the resonance frequencies is stronger for the lighter molecular ions (H_2^+).

The upward shift is clearly seen in Fig. 1(c), for the Be^+-$^4He^+$ crystal. From the experimental data we extrapolate a value of ≈675 kHz for zero excitation amplitude (calculated single-particle frequency 630 kHz). This shift is caused by the Coulomb interaction between the Be^+ body of the crystal and the He^+ core, and is confirmed by the MD simulations. The presence of the Coulomb potential of the core ions "steepens" the effective potential in which the beryllium ions move (when added to the harmonic trapping potential). Likewise, the outer beryllium shells' Coulomb potential increases the effective harmonic frequency (to a first approximation) confining the core ions. The reason this is not observed for pure crystals (inner shells altering the frequency of outer shells) is that they all oscillate coherently when driven by an external potential, and so the ion's Coulomb potential moves with them—no ion experiences significant deviation from its equilibrium position in the crystal, although the crystal as a whole is moving. When two species, with different motional frequencies, are present this is no longer true—each moves in the Coulomb potential of the other. The size of the induced secular frequency shifts is also confirmed by our MD simulations [Fig. 1(d)].

The amplitudes of the resonances in Fig. 3(b) indicate that (approximately) the number of H_3^+ ions exceeds the number of H_2^+ ions by a factor of 2. Using other loading procedures, e.g., varying the loading time or the partial pressure of the neutral H_2 gas, different relative fractions between the individual core constituents were achieved, and thus different coupling strengths were observed. For crystals with varying ion fractions in the core, the comparison between experimental and simulated spectra allows for an estimate of their relative fractions, even when the individual features are not resolved, whereas the total LC and SC ion numbers are determined by comparison between the CCD images observed and the simulated crystal shapes [9,19,26].

C. Asymmetry

The axial symmetry of the effective potential is broken when a static (quadrupole) potential is applied to the trap, so that the different ion species are displaced from the trap center. The displacement is larger for heavier (less tightly bound) species. In this way one can achieve a configuration in which lighter SC ion species are located outside the beryllium ion shell ensemble.

Figure 5 shows observed secular frequency spectra [Figs. 5(b) and 5(f)] for different asymmetric mixed-species ion crystals [Figs. 5(a) and 5(c)]. In Figs. 5(d)–5(f), the results of MD simulations for the ion crystal in Fig. 5(c) together with the corresponding simulated secular frequency spectrum are presented, respectively.

For mixed-species ion crystals with at least three components in an asymmetric potential, the secular spectrum at low

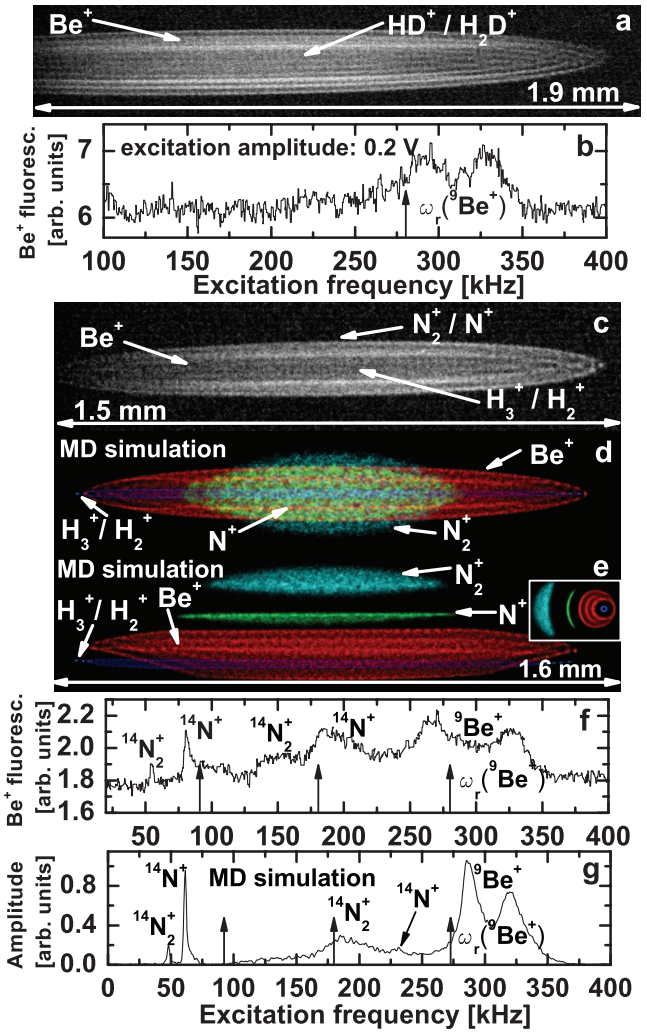

FIG. 5. (Color online) Trap-asymmetry-induced frequency shifts. (a) Asymmetric Be^+ ion crystal containing ≈3220 Be^+, ≈250 H_2D^+, and ≈250 HD^+ ions at ≈30 mK (dark core). (b) High-mass motional spectrum of the crystal in (a). (c) Asymmetric Be^+ ion crystal, after loading with H_2 gas. The crystal contains ≈900 Be^+, ≈90 H_3^+, ≈90 H_2^+, ≈50 N^+, and ≈100 N_2^+ at 20 mK. Relative fractions of H_2^+ and H_3^+ ions are estimated from corresponding secular spectra. (d), (e) MD simulation of the crystal in (c). The view is from the side (d), same perspective as in (c), from the top (e) (in the plane and perpendicular to the plane of observation of the camera, respectively), and along the axis of the trap, inset in (e). Individual ion species are spatially shifted relative to each other and relative to the trap center, due to trap potential anisotropy. (f) High-mass motional spectrum of the crystal in (c). (g) Simulated secular frequency spectrum for the crystal in (d). Vertical arrows mark the calculated single-particle frequencies of N_2^+ (90 kHz), N^+ (180 kHz), and Be^+ (280 kHz).

excitation frequencies can be complex. In the absence of heavier molecular ions, usually embedded outside the Be^+ ion shells, the secular frequency for the Be^+ ions usually is split in frequency and shifted to slightly higher frequencies, due to Coulomb coupling to the large number of light molecular species embedded in the crystal core [Figs. 5(a) and 5(b)].

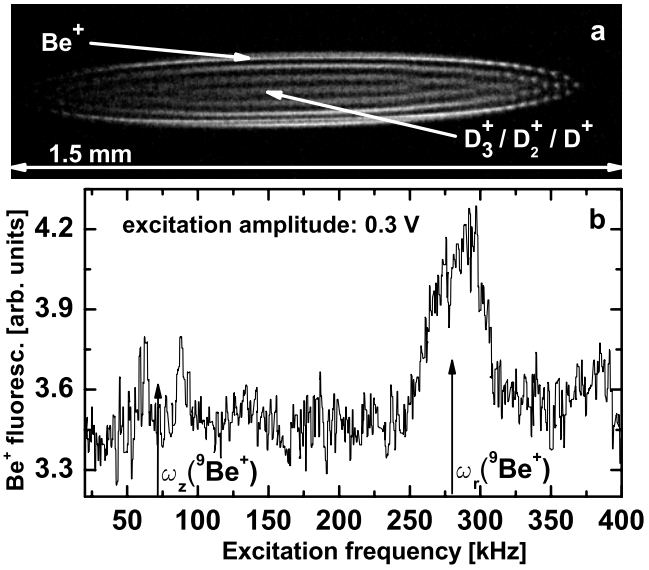

FIG. 6. Excitation of axial trap modes in an asymmetric trap potential. (a) Asymmetric mixed-species ion crystal containing 700 Be^+ and 550 lighter SC ions, D_3^+, D_2^+, and D^+, at ≈20 mK. Heavier molecular ions were removed from the trap. (b) High-mass motional spectrum of the crystal in (a). Measured resonances are attributed to the excitation of axial (at 63 and 88 kHz) and radial (at around 285 kHz) Be^+ trap modes. The calculated axial (71 kHz) and radial (280 kHz) single-particle frequencies for Be^+ are marked with arrows.

In the presence of heavier ions (and of a light core) [see Figs. 5(c) and 5(f)], the beryllium resonance is also split in frequency (peaks at 265 and 330 kHz). Its calculated single-particle frequency is at 280 kHz. Additional peaks at 190, at 150, at 81, and at 54 kHz are present. These resonances are caused by heavier contaminants present in the trap: N^+ ions (at 81 and 190 kHz) and N_2^+ ions (at 54 and 150 kHz), again split in frequency due to the anisotropy of the trap potential. The calculated single-particle frequencies are at 90 (for N_2^+) and 180 kHz (for N^+).

In addition, we observed experimentally that in the presence of a heavier or lighter species outside the beryllium crystal (possible for asymmetric crystals), and/or in the presence of a strong cooling light-pressure force on the beryllium ions (which moves the beryllium ions to one end of the crystal) in an asymmetric trap potential, the radial excitation of the heavy or light ions in the outer crystal regions can couple into the z motion of the beryllium. As the outer (heavy or light) ions are moved radially, the beryllium is displaced along z, and so its axial motion is excited. A mixed-species ion crystal and the corresponding motional spectrum illustrating this effect are shown in Figs. 6(a) and 6(b), respectively. In the spectrum, we found that the axial Be^+ resonance is split in frequency (due to the trap anisotropy) and that the radial Be^+ resonance is broadened compared to the unperturbed situation. Furthermore, the axial and radial resonances are centered around slightly larger frequencies compared to the calculated single-particle frequencies. This is attributed to Coulomb-coupling-induced frequency shifts in the mixed-species ion crystal. The excitation of the axial

resonances is not present if the SC ions are expelled from the trap or the asymmetry of the trap potential is removed.

In the special case of the spectrum shown in Fig. 5(f) the Be^+ axial resonance (possibly split in frequency) is probably hidden under the larger features caused by N_2^+ and N^+ ions. We expect that a systematic study of the above axial excitation of beryllium trap modes will be necessary for better characterization of the underlying mechanisms. Note that we did not observe shifts of the secular frequencies of lighter molecular ions inside or outside the Be^+ crystal for anisotropic trap potentials (i.e., when the symmetry of the trap potential was broken by suitable static offset potentials) compared to the isotropic case.

Furthermore, as confirmed by our simulations, a common mode of oscillation between Be^+ and heavier impurity ions, e.g., N^+, could contribute to the resonance at around 150 kHz in Fig. 5(f), which in this case is dominated by the N_2^+ resonance and which is not observed when such a crystal is symmetrized, and/or after removal of the heavier ions from the trap [see also Figs. 5(a) and 5(b)]. After symmetrization of the trap potential (i.e., placing the dark core containing the molecular ions in the trap center), the frequency splitting of the axial and radial Be^+ resonances ω_z and ω_r is also absent.

Figures 5(d)–5(f) show results obtained from MD simulations for the crystal in 5(c) together with the corresponding simulated secular spectrum. As obvious from Figs. 5(d) and 5(e) the ion species are spatially separated, due to the trap potential anisotropy. The simulated spectrum in Fig. 5(g) is in reasonable overall agreement with the experimental result [Fig. 5(f)]. However, the detailed positions of the features in the simulated spectrum deviate from the experimental data. The individual features identified in Fig. 5(g) are at 285 and at 320 kHz (Be^+ ions), at 61 and at 232 kHz (N^+ ions), and at 48 and at 188 kHz (N_2^+ ions). The simulations show that the position and size of the individual features depend strongly on the ion numbers involved and the size of the electric fields causing the trap anisotropy. Using the various ion numbers as fit parameters in the simulations, the agreement between experimental and theoretical spectra could be improved. Thus, an accurate experimental determination of the ion numbers, e.g., by ion extraction and counting, would improve the accuracy of the simulated spectra.

VIII. SUMMARY

In this work, we investigated the motional resonance spectrum of multispecies ion crystals (up to four species) in a linear Paul trap, for both isotropic and anisotropic trap potentials. The coupling between different motional resonances was studied experimentally and theoretically (by MD simulations), in order to interpret the complicated trap mode spectra measured and to reliably identify sympathetically cooled particle species, even when individual secular resonances cannot be resolved and/or direct (fluorescence) detection is prevented. We have shown that the simulations are essential for the interpretation of the experimental spectra, which are complicated by the fact that the observed resonance frequencies and their coupling are usually determined by the superposition of several, sometimes opposing, line shifting effects. In the MD simulations the different frequency shifting effects contributing to the spectra were modeled and their interplay was studied. The simulated spectra faithfully reproduce the experimental results. Quantitative agreement can be achieved using the ion numbers in the simulations as fit parameters, thus allowing for an accurate determination of relative ion species numbers contained in a given crystal. We have observed that the spectra become more complicated as the number of species increases and the lines broaden as the ion numbers increase. Further studies should explore the mode spectra of crystals containing five or more species and the mechanisms leading to the axial excitation of the beryllium ion modes.

ACKNOWLEDGMENTS

We thank H. Wenz and C. B. Zhang for the MD simulations and the Deutsche Forschungsgemeinschaft (DFG) and the EC network HPRN-CT-2002-00290 for financial support. P. B. was also supported by the Alexander von Humboldt Stiftung.

[1] S. G. Karshenboim and V. G. Ivanov, Eur. Phys. J. D **19**, 13 (2002).
[2] S. Schiller and V. I. Korobov, Phys. Rev. A **71**, 032505 (2005).
[3] M. Greiner, C. A. Regal, and D. S. Jin, Phys. Rev. Lett. **92**, 040403 (2004).
[4] S. Dürr *et al.*, Phys. Rev. Lett. **92**, 020406 (2004).
[5] A. Fioretti *et al.*, Phys. Rev. Lett. **80**, 4402 (1998).
[6] J. D. Weinstein *et al.*, Nature (London) **395**, 148 (1998).
[7] S. A. Rangwala *et al.*, Phys. Rev. A **67**, 043406 (2003).
[8] K. Molhave and M. Drewsen, Phys. Rev. A **62**, 011401(R) (2000).
[9] P. Blythe, B. Roth, U. Fröhlich, H. Wenz, and S. Schiller, Phys. Rev. Lett. **95**, 183002 (2005).
[10] M. Welling *et al.*, Int. J. Mass Spectrom. Ion Process. **172**, 95 (1998).
[11] T. Baba and I. Waki, J. Appl. Phys. **89**, 4592 (2001).
[12] M. Drewsen *et al.*, Phys. Rev. Lett. **93**, 243201 (2004).
[13] H. Schnitzler *et al.*, Appl. Opt. **41**, 7000 (2002).
[14] D. J. Larson *et al.*, Phys. Rev. Lett. **57**, 70 (1986).
[15] F. Diedrich *et al.*, Phys. Rev. Lett. **59**, 2931 (1987).
[16] B. Roth, U. Fröhlich, and S. Schiller, Phys. Rev. Lett. **94**, 053001 (2005).
[17] U. Fröhlich, B. Roth, and S. Schiller, Phys. Plasmas **12**, 073506 (2005).
[18] T. Baba and I. Waki, Jpn. J. Appl. Phys., Part 1 **92**, 4109 (2002).
[19] B. Roth, A. Ostendorf, H. Wenz, and S. Schiller, J. Phys. B **38**, 3673 (2005).
[20] E. W. McDaniel, V. Cermak, A. Dalgarno, E. E. Ferguson, and

L. Friedman, *Ion-Molecule Reactions* (John Wiley & Sons, New York, 1970).
[21] K. P. Huber and G. Herzberg, *Molecular Spectra and Molecular Structure* (Van Nostrand–Reinhold, New York, 1979).
[22] M. T. Bowers and D. E. Elleman, J. Chem. Phys. **51**, 4606 (1969).
[23] D. H. E. Dubin and T. M. O'Neil, Rev. Mod. Phys. **71**, 87 (1999).
[24] B. Roth, J. Koelemeij, H. Daerr, and S. Schiller, Phys. Rev. A **74**, 040501(R) (2006).
[25] B. Roth, P. Blythe, H. Wenz, H. Daerr, and S. Schiller, Phys. Rev. A **73**, 042712 (2006).
[26] B. Roth, H. Daerr, P. Blythe, L. Patacchini, and S. Schiller, J. Phys. B **39**, S1241 (2006).
[27] T. Hasegawa and T. Shimizu, Phys. Rev. A **66**, 063404 (2002).